

SLIM : ONE-SHOT QUANTIZED SPARSE PLUS LOW-RANK APPROXIMATION OF LLMs

Mohammad Mozaffari

Department of Compute Science
University of Toronto
mmozaaffari@cs.toronto.edu

Maryam Mehri Dehnavi

Department of Compute Science
University of Toronto
mmehride@cs.toronto.edu

ABSTRACT

Large Language Models (LLMs) have revolutionized natural language understanding and generation tasks but suffer from high memory consumption and slow inference times due to their large parameter sizes. Traditional model compression techniques, such as quantization and pruning, mitigate these issues but often require retraining to maintain accuracy, which is computationally expensive. This paper introduces SLIM, a novel approach for compressing LLMs using a one-shot Quantized Sparse Plus Low-rank Approximation. SLIM eliminates the need for costly retraining by combining a symmetric quantization method (SLIM-Quant) with a saliency-based low-rank approximation. Our method reduces quantization error while leveraging sparse representations compatible with accelerated hardware architectures. Additionally, we propose a parameter-efficient fine-tuning recipe that significantly reduces overhead compared to conventional quantization-aware training. SLIM achieves up to a 5.4% improvement in model accuracy for sparsity patterns like 2:4, and the fine-tuning step further enhances accuracy by up to 5.8%, demonstrating state-of-the-art performance. This work provides a pathway for efficiently deploying large models in memory-constrained environments without compromising accuracy.¹

1 INTRODUCTION

Large Language Models (LLMs) (Brown et al., 2020; Radford et al., 2019) are transformative for natural language understanding and generation (Suzgun et al., 2022; Zhou et al., 2023); however, their extensive parameter count leads to large memory footprints and longer inference times, making them expensive to execute. Model compression methods, such as sparsity and quantization, have shown promising results in reducing the inference costs of LLMs. However, these methods often require costly retraining on large amounts of data to restore the original model accuracy (Sanh et al., 2020; Park et al., 2018), while facing numerical and optimization stability challenges when dealing with quantized weights in quantization-aware-training (Gholami et al., 2022).

To address these issues, one-shot pruning methods have emerged, eliminating the need for the retraining. They achieve high accuracy using only a small set of calibration data. Optimal Brain Damage (OBD) (LeCun et al., 1989) pioneered the use of second-order information of the loss function for model compression (Singh & Alistarh, 2020; Mozaffari et al., 2023), though at a high computational cost. Subsequent methods like Optimal Brain Surgeon (OBS) (Hassibi et al., 1993) and modern approaches such as SparseGPT (Frantar & Alistarh, 2023) and WANDA (Sun et al., 2023) build on these ideas, and introduce computationally feasible alternatives for LLMs. While these methods perform well with unstructured sparsity, they struggle with semi-structured sparsity patterns like the NVIDIA 2:4 sparsity pattern (Mishra et al., 2021), which are necessary for hardware-accelerated inference.

Post-training quantization (Rokh et al., 2023) methods are an effective compression strategy for reducing both memory usage and computation costs. SmoothQuant (Xiao et al., 2023) preserves accuracy by leaving the more salient weight channels unquantized, but this results in inefficient de-

¹Code and data for SLIM is available at: <https://github.com/Mohammad-Mozaffari/slim>

quantization during inference. AWQ (Lin et al., 2024) addresses this by scaling the salient weight channels and adjusting the input channels accordingly. However, this introduces irregular memory access patterns during input scaling and causes inaccuracies in input quantization, limiting AWQ to weight-only quantization. OPTQ (or GPTQ) (Frantar et al., 2022), a leading quantization method, reduces quantization error by adjusting weight values after quantizing a subset of the weights. All these methods employ group quantization (Alistarh et al., 2017; Gunho et al., 2022), where quantization parameters are shared across weight groups instead of individual elements. Although group quantization reduces quantization error, it increases computational and memory overhead during inference and requires custom CUDA functions for efficient dequantization.

While sparsity and quantization individually offer substantial reductions in model size and inference cost, combining these techniques holds even greater potential for compressing large models (Frantar & Alistarh, 2023). However, combining sparsity and quantization often exacerbates the accuracy loss from each method, resulting in a substantial performance gap between the compressed model and the original model. This accuracy gap highlights the need for further innovations in compression techniques. Recent work has aimed to reduce compression error by using learnable low-rank adapters to minimize weight reconstruction error (Guo et al., 2023; Nikdan et al., 2024), followed by an expensive fine-tuning step on hundreds of millions of tokens (Dettmers et al., 2023; Li et al., 2023). This prolonged fine-tuning is necessary because the low-rank adapters do not account for the saliency of the weights at initialization (Dettmers et al., 2023; Guo et al., 2023).

To address these limitations, we propose a saliency-based one-shot low-rank approximation that mitigates the accuracy loss caused by quantization and sparsity. Saliency-based methods require weights to remain static during quantization and pruning, which renders approaches like OPTQ and SparseGPT ineffective. To resolve this, we introduce a novel symmetric weight quantization scheme that not only effectively reduces quantization error but is also compatible with saliency-based methods. We complement our quantizer and low-rank adapters with an optional light-weight fine-tuning recipe that can further boost the accuracy of the models using only 300,000 tokens.

Our method, SLiM, is a One-shot Quantized Sparse Plus Low-rank Approximation of LLMs. Key contributions of SLiM are:

- **SLiM-Quant:** We propose a symmetric weight quantization scheme that minimizes the Frobenius norm of quantization error without altering the weights, making it compatible with saliency-based pruning and low-rank approximation methods. Unlike group quantization, SLiM-Quant uses a single parameter for the entire weight matrix, reducing computational and memory overhead and simplifying implementation.
- **Saliency-based One-shot Low-rank Adapters:** We introduce a one-shot low-rank adapter method that minimizes accuracy loss by reconstructing weights based on their saliency, targeting weights with the highest impact on model output.
- **Parameter-Efficient Fine-tuning:** We propose a fine-tuning recipe for sparse, quantized models that avoids the complexities of quantization-aware training while drastically reducing fine-tuning time. For example, fine-tuning a 13B parameter model, which typically takes up to 36 days, is reduced to just 14 hours on a single H100 GPU.
- **Accuracy Gains:** SLiM improves model accuracy by up to 5.4% (LLaMA-2-7B) over state-of-the-art pruning and quantization methods (SparseGPT + Group OPTQ) for 2:4 sparsity. With our parameter-efficient fine-tuning, the gap widens to 5.8% (LLaMA-2-13B).

2 PRELIMINARIES

Optimal Brain Surgeon. The primary objective in model compression is to minimize the output discrepancy between the compressed models and the original models. Optimal Brain Surgeon (Hasibi et al., 1993) simplifies this approach by minimizing the output difference at each network layer over a calibration dataset. Consider a single feed-forward layer with input $\mathcal{X} \in \mathbb{R}^{b \times d_{in}}$, weight $\mathcal{W} \in \mathbb{R}^{d_{in} \times d_{out}}$, and output $\mathcal{Y} \in \mathbb{R}^{b \times d_{out}}$, where b , d_{in} , and d_{out} represent the batch size, input hidden dimension, and output hidden dimension, respectively. Denoting the compressed matrices with a superscript C , OBS aims to minimize Equation 1. This formulation allows OBS to focus on maintaining layer-wise fidelity during compression, potentially leading to better overall model performance.

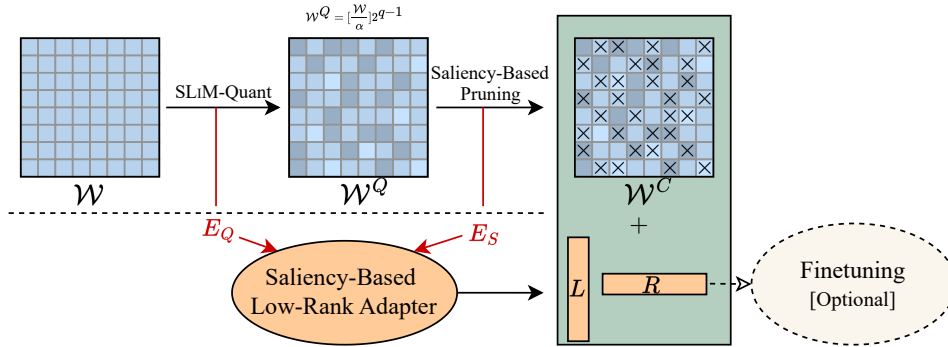


Figure 1: Figure 1: SLiM weight compression pipeline. The process involves: (1) Quantizing weights using the symmetric SLiM-Quant algorithm (generating quantized weight \mathcal{W}^Q and quantization error E_Q); (2) Sparsifying quantized weights through saliency-based pruning (generating compressed weight \mathcal{W}^C with sparsity error E_S); (3) Compensating for quantization and sparsity errors via SLiM saliency-based low-rank approximation (generating left and right low-rank adapters L and R). Optionally, adapters can undergo fine-tuning to further improve model accuracy while keeping sparse quantized weights frozen.

$$\min_{\mathcal{W}^C} |\mathcal{Y}^C - \mathcal{Y}|^2 = \min_{\mathcal{W}^C} |\mathcal{X}(\mathcal{W} - \mathcal{W}^C)|^2 \quad (1)$$

Considering Equation 1, Wanda (Sun et al., 2023) proposes a saliency matrix \mathcal{S} to evaluate the importance of each parameter. This matrix is defined as $\mathcal{S} = \mathbf{x}^T \odot \mathcal{W}$, where $\mathbf{x} \in \mathbb{R}^{d_{in} \times 1}$ represents the average absolute value of each input, \odot denotes element-wise multiplication, and $|\cdot|$ represents the absolute value operator. SLiM adopts this same metric to assess the importance of different weights and determine the sparsity patterns in the sparse weight representation.

Symmetric Quantization. Symmetric quantization, the simplest form of quantization, computes $\mathcal{M}^Q \propto \text{round}(\frac{\mathcal{M}}{\alpha})$, where \mathcal{M}^Q is the quantized matrix and α is the quantization parameter. This method effectively accelerates matrix multiplications, as dequantization of the output requires only a scalar multiplication.

AbsMax (Jacob et al., 2018), the most common symmetric quantization method, sets α to the maximum absolute value in the matrix. However, AbsMax is sensitive to outliers, which can significantly alter α , thereby reducing quantization precision. For zero-centered bell-curved distributions typical of LLM weights and inputs, AbsMax maps a large portion of weights to zero, resulting in high error values.

Group quantization Alistarh et al. (2017); Gunho et al. (2022) addresses this issue by sharing the quantization parameter among fewer elements in the weight matrix. This approach divides the weight matrix into smaller subgroups, each quantized with its own scaling factor. While this allows for more fine-grained representation of weight distributions and better captures local variations in weight magnitudes, it introduces memory overheads and complicates dequantization methods. Specifically, group quantization increases memory usage and computational complexity in exchange for potentially improved quantization accuracy.

3 QUANTIZED SPARSE PLUS LOW-RANK APPROXIMATION OF LLMs

To effectively apply quantization, sparsity, and low-rank adapters to LLMs, SLiM introduces a novel quantization scheme called SLiM-Quant. This method reduces quantization error and is followed by pruning the quantized model using the importance metric proposed in Section 2. Subsequently, SLiM adds low-rank adapters to minimize the saliency of the compression error introduced by sparsity and quantization. Figure 1 illustrates this process. In the following subsections steps in this approach are explained.

3.1 SLIM QUANTIZATION METHOD

SLIM focuses on symmetric weight quantization due to its low dequantization and memory overhead and ease of implementation. Denoting the quantized matrices by Q superscript, Equation 2 shows the symmetric quantization formula for q -bit quantization, where α is the quantization parameter and $clip(\cdot)$ operator clips the input to values between $[-1, 1]$.

$$\mathcal{W}^Q = \text{round}(\text{clip}(\frac{\mathcal{W}}{\alpha}))2^{q-1} \quad (2)$$

The objective of quantization is to reduce the weight reconstruction error shown in Equation 3, where the $*$ superscript shows the optimal value. But the objective function in Equation 3 is not convex, and to our best knowledge, does not have a closed form solution.

$$\alpha^* = \arg \min_{\alpha} \|\mathcal{W}^Q - \mathcal{W}\|^2 = \arg \min_{\alpha} \|\text{round}(\text{clip}(\frac{\mathcal{W}}{\alpha}))2^{q-1} - \mathcal{W}\|^2 \quad (3)$$

To solve the mean squared error (MSE) problem in Equation 3, we propose a probabilistic reformulation as shown in Equation 4, where $Q(\cdot)$ and $Q^{-1}(\cdot)$ are the quantization and dequantization functions respectively and $f(\cdot)$ is the probability distribution function (PDF) of the weight elements.

$$\alpha^* = \arg \min_{\alpha} \|\mathcal{W}^Q - \mathcal{W}\|^2 = \arg \min_{\alpha} \int_{-\infty}^{\infty} f(x) |Q^{-1}(Q(x)) - x|^2 dx \quad (4)$$

By incorporating the quantization formula from Equation 2 into Equation 4, we can simplify the integration into the sum of two terms based on the absolute value of the data: the quantization error for absolute values less than α (Equation 5) and the clipping error for absolute values larger than α (Equation 6). Here, $f_{abs}(\cdot)$ represents the probability density function (PDF) of the absolute value of the weights. Equation 7 presents the simplified version of Equation 4.

$$E_{quant}(\alpha) = \int_0^{\alpha} f_{abs}(x) |\alpha \times \text{round}(\frac{x}{\alpha}) \times 2^{1-q} - x|^2 dx \quad (5)$$

$$E_{clip}(\alpha) = \int_{\alpha}^{\infty} f_{abs}(x) |\alpha - x|^2 dx \quad (6)$$

$$\alpha^* = \arg \min_{\alpha} E_Q(\alpha) = \arg \min_{\alpha} E_{quant}(\alpha) + E_{clip}(\alpha) \quad (7)$$

Equation 7 can theoretically be solved by differentiating the objective function with respect to α , assuming the probability density function (PDF) of the distribution is known. However, in practice, neural network weight distributions don't follow standard distributions. We tested models like Gaussian, Laplace, Pareto, q-Gaussian, and Weibull, but none fit the observed weight distributions, highlighting their uniqueness.

To overcome the lack of a closed-form weight PDF, we use numerical integration over the weight histogram to solve Equation 7. We implement a multi-grid approach to optimize efficiency, starting with 10 uniform samples in the range $(0, \max(W))$ and iteratively refining around the minimum error to find the optimal α . The full method is detailed in Algorithm 1.

3.2 SLIM LOW-RANK ADAPTERS

The effects of quantization and pruning of a weight matrix can be modeled as additive noise, such that $\mathcal{W}^C = \mathcal{W} + E_Q + E_S$, where E_Q and E_S are the quantization and sparsity errors respectively. We aim to add low-rank adapters to the weights that cancel the compression errors, i.e. $\mathcal{W} \approx \mathcal{W}^C + \mathcal{LR}$, where $\mathcal{L} \in \mathbb{R}^{d_{in} \times r}$ and $\mathcal{R} \in \mathbb{R}^{r \times d_{out}}$ are the low-rank adapters and r is the adapter rank.

Algorithm 1 SLIM-Quant Algorithm

```

1: Input: Weight Magnitude PDF:  $f_{abs}$ , High Resolution Step Size:  $\eta_{high}$ , Low Resolution Step
   Size:  $\eta_{low}$  Weight Matrix:  $\mathcal{W}$ , Quantization Bitwidth:  $q$ 
2: Output:  $\mathcal{W}_{quant}$ 
3: procedure ESTIMATEERROR( $\alpha$ )
4:    $E_{quant}(\alpha) = \int_0^\alpha f_{abs}(x) |\alpha \times \text{round}(\frac{x}{\alpha}) \times 2^{1-q} - x|^2 dx$ 
5:    $E_{clip}(\alpha) = \int_\alpha^\infty f_{abs}(x) |\alpha - x|^2 dx$ 
6:   return  $E_{quant} + E_{clip}$ 
7:  $E = \text{EmptyDictionary}()$ 
8: for  $\alpha$  in range(0,  $M$ ,  $\eta_{low}$ ) do
9:    $E(\alpha) = \text{ESTIMATEERROR}(\alpha)$ 
10:  $\alpha_{low} = \arg \min_\alpha E(\alpha)$ 
11: for  $\alpha$  in range( $\alpha_{low} - \eta_{low}$ ,  $\alpha_{low} + \eta_{low}$ ,  $\eta_{high}$ ) do
12:    $E(\alpha) = \text{ESTIMATEERROR}(\alpha)$ 
13:  $\alpha^* = \arg \min_\alpha E(\alpha)$ 
14:  $\mathcal{W}_{quant} = \text{round}(\text{clip}(\frac{\mathcal{W}}{\alpha^*})) \times 2^{q-1}$ 

```

Naively, one can try to minimize the total error norm between \mathcal{W} and \mathcal{W}^C . In this approach, the magnitude of the error is the minimization objective, and the importance of different weights are not taken into account. Similar to magnitude pruning, this approach results in low model accuracy as discussed in Section 4.

We propose a new formulation to incorporate the weight saliency into the low-rank approximation, and then utilize the proper saliency function to find the optimal adapters in practice. Assuming that there exists an additive invertible saliency function $F: \mathbb{R}^{d_{in} \times d_{out}} \rightarrow \mathbb{R}^{d_{in} \times d_{out}}$, solving Equation 8, in which we have used the additive property of F and the fact that $F(\mathcal{W}) < F(\mathcal{W}^C + (LR))$.

$$\mathcal{L}, \mathcal{R} = \arg \max_{\mathcal{L}, \mathcal{R}} \|F(\mathcal{W}^C + \mathcal{L}\mathcal{R})\|^2 = \arg \min_{\mathcal{L}, \mathcal{R}} \|F(\mathcal{W} - (\mathcal{W}^C + \mathcal{L}\mathcal{R}))\|^2 \quad (8)$$

By using the additive feature of the saliency function $F(\cdot)$, we can simplify Equation 8 to Equation 9. By solving the optimization problem in equation 9, we can obtain the optimal low-rank adapters.

$$\mathcal{L}, \mathcal{R} = \arg \min_{\mathcal{L}, \mathcal{R}} \|F(\mathcal{W} - \mathcal{W}^C) - F(\mathcal{L}\mathcal{R})\|^2 = \arg \min_{\mathcal{L}, \mathcal{R}} \|F(-(E_Q + E_S)) - F(\mathcal{L}\mathcal{R})\|^2 \quad (9)$$

For solving the optimization problem in Equation 9, we replace $F(\cdot)$ with the saliency function discussed in section 2, i.e. $F(\mathcal{W}) = \mathbf{x}^T \odot \mathcal{W}$, where $\mathbf{x} \in \mathbb{R}^{d_{in} \times 1}$ represents the average absolute value of inputs from a calibration set. For simplicity, we use matrix multiplications instead of element-wise multiplication, resulting in Equation 10.

$$F(\mathcal{W}) = \text{diag}(\mathbf{x})\mathcal{W} \quad (10)$$

Replacing Equation 10 in the objective function in Equation 9, Equation 11 is obtained, which can be solved by a singular value decomposition and a matrix inversion on the left low-rank adapter, as in Equation 12.

$$\mathcal{L}, \mathcal{R} = \arg \min_{\mathcal{L}, \mathcal{R}} \| -\text{diag}(\mathbf{x})(E_Q + E_S) - \text{diag}(\mathbf{x})\mathcal{L}\mathcal{R} \|^2 \quad (11)$$

$$\text{diag}(\mathbf{x})\mathcal{L}, \mathcal{R} = -\text{SVD}(\text{diag}(\mathbf{x})(E_Q + E_S)) \quad (12)$$

Please note that the invertibility of the saliency function in Equation 10 is dependent on the invertibility of $\text{diag}(\mathbf{x})$, which in turn requires all values in \mathbf{x} to be not equal to zero. But in practice, due to the limited numerical range and the non-linearities such as ReLU in LLMs, $\text{diag}(\mathbf{x})$ can become

Algorithm 2 SLiM Saliency-based Low-rank Adapter Computation

-
- 1: **Input:** Original Weight: \mathcal{W} , Compressed Weight: \mathcal{W}^C Calibration Input: \mathcal{X}
 - 2: **Output:** \mathcal{L}, \mathcal{R} : Saliency-based Low-rank Adapters
 - 3: $E_C = E_Q + E_S = \mathcal{W}^C - \mathcal{W}$ // Compute compression Error
 - 4: $\tilde{\mathbf{x}} = \text{mean}(\mathcal{X})$ // Average over all the samples
 - 5: $\mathbf{x} = \tilde{\mathbf{x}} + \min(|\tilde{\mathbf{x}}|)$ // Shift all the values to avoid zeros in \mathbf{x}
 - 6: $\mathcal{S}_C = \text{diag}(\mathbf{x})E_C$ // Compute compression error saliency
 - 7: $\tilde{\mathcal{L}}, \tilde{\mathcal{R}} = \text{SVD}(\mathcal{S}_C)$ // Low-rank approximation of compression error saliency
 - 8: $\mathcal{L} = \text{diag}(1/\mathbf{x})\tilde{\mathcal{L}}, \mathcal{R} = \tilde{\mathcal{R}}$ // Converting saliency factors to weight factors
-

singular. To avoid such cases. This behavior will also lead to having the rows of the saliency matrix to be set to zero, not distinguishing between the less and more important weights in a row. To overcome these challenges, we have added the minimum absolute value available in \mathbf{x} to all its elements. Algorithm 2 summarizes all the details of computing the saliency-based low-rank adapters in SLiM.

3.3 POST-COMPRESSION FINE-TUNING

Fine-tuning models after applying one-shot compression presents significant challenges, primarily due to the limitations imposed by the integer representation of parameters in quantized weights. Quantized weights have limited precision and restricted value ranges, making gradient-based updates difficult and potentially leading to loss of information during fine-tuning. Moreover, the high parameter count of large language models renders traditional fine-tuning extremely computationally expensive and time-consuming, necessitating more parameter-efficient methods.

SLiM addresses these issues by introducing fine-tunable parameters in the form of low-rank adapters. In its optional fine-tuning phase, SLiM freezes the sparse and quantized weights, allowing only the tuning of these low-rank adapters. This parameter-efficient fine-tuning approach enables rapid improvement in the compressed model’s accuracy using a short fine-tuning phase over just thousands of tokens. By focusing the fine-tuning process on a small subset of parameters (the adapters), SLiM significantly reduces the computational requirements while still allowing the model to adapt to new data or tasks. This approach strikes a balance between maintaining the benefits of compression and enabling post-compression adaptation.

3.4 TILED LOW-RANK ADAPTER QUANTIZATION

Pruning and quantizing the weights reduces the computation and memory footprint of the models significantly ($\sim 8\times$ reduction in memory size), but adding low-rank adapters in full precision will result in an extra overhead. To reduce the adapter overheads, we compress the adapters using quantization. The distribution of the elements in the factors have long tails, making even advanced methods that don’t use group quantization such as SLiM-Quant impractical. On the other hand, available group quantization methods use 1-dimensional tiles for quantization, which does not match the layout used for tensor cores, hence making them not hardware-friendly.

To address these issues, we propose a tiled quantization scheme for the low-rank adapters, in which 256 elements of the adapter are quantized using the same quantization parameter, creating 16×16 tiles. The choice of 16×16 blocks is made based on the input size of tensor cores in NVIDIA A100 and H100 GPUs, making it the tiling strategy more hardware friendly and allowing the warps in the GPU to dequantize the data in for different tensor cores in parallel using only one quantization parameter per tensor core. The quantization of each tile is done using the AbsMax algorithm.

4 EXPERIMENTAL RESULTS

Models, Datasets, and Evaluation. We evaluate SLiM on the OPT (Zhang et al., 2022) and LLaMA-2 (Touvron et al., 2023) model families, both of which serve as standard baselines in model compression studies (Frantar et al., 2022; Frantar & Alistarh, 2023; Sun et al., 2023). Model accuracy is assessed on a range of zero-shot downstream tasks, including MMLU (Hendrycks et al.,

2020), Piqa (Bisk et al., 2020), Arc-Easy, Arc-Challenge (Clark et al., 2018), WinoGrande (Sakaguchi et al., 2021), and OpenBookQA (Mihaylov et al., 2018). For zero-shot evaluations, we utilize the Language Model Evaluation Harness (Gao et al., 2024) framework. In line with prior work (Sun et al., 2023; Frantar & Alistarh, 2023; Frantar et al., 2022), we also report the perplexity of the models on a language modeling task on the WikiText2 (Merity et al., 2016) dataset, provided in Appendix A.

Baselines. We compare SLiM against state-of-the-art one-shot pruning methods, including Wanda (Sun et al., 2023), SparseGPT (Frantar & Alistarh, 2023), and Magnitude Pruning (Han et al., 2015), as well as one-shot quantization techniques like OPTQ (Frantar et al., 2022) and AbsMax. Since AWQ (Lin et al., 2024) relies on floating point activations, we have not included it in our experiments, in which both weights and activations are quantized.

Similar to other leading one-shot pruning and quantization methods (Wanda, SparseGPT, OPTQ), SLiM leverages calibration data to extract statistics and assess weight saliency. As Wanda, SparseGPT, and OPTQ operate under identical conditions, we adopt their approach, using 128 sequences sampled from the C4 (Raffel et al., 2019) dataset. Additionally, for all fine-tuning experiments, we utilize 300,000 tokens from the C4 dataset.

Sparse and Quantized. We evaluate model accuracy across structured and unstructured sparsity benchmarks for various pruning and quantization methods. Specifically, we pair OPTQ and SparseGPT, which follow similar error recovery strategies, and combine Wanda with AbsMax and SLiM-Quant, while using Magnitude Pruning with AbsMax. To demonstrate the effectiveness of SLiM saliency-based low-rank adapters, we introduce low-rank adapters to Wanda, minimizing the magnitude of the error (rather than the saliency) using SVD. This approach, referred to as the "SVD low-rank adapter or Wanda-SVD" in the tables, is similar to LQLoRA (Guo et al., 2023) with the difference that LQLoRA does not prune the weights, nor uses SLiM-Quant for quantization, leading to significantly higher error rates. We do not apply one-shot low-rank adapters to SparseGPT or OPTQ, as their weight update rules conflict with minimizing weight error. Additionally, for a more thorough experiment setting, we have implemented group quantization for AbsMax, and have tested it with different settings.

Table 1 presents the zero-shot task accuracy results for sparse and quantized versions of the OPT and LLaMA-2 models. Among the tested methods, Magnitude Pruning combined with AbsMax quantization yields the lowest accuracy, with AbsMax applied to Wanda showing similarly poor performance. While applying SLiM-Quant to Wanda alleviates some of the accuracy loss, it still falls short compared to SparseGPT and OPTQ. In contrast, SLiM achieves the highest accuracy across all methods, with further improvements gained through a brief fine-tuning step (SLiM + FT). Additionally, SLiM^Q quantizes the low-rank adapters to 4 bits, reducing adapter overhead by 4× while maintaining competitive accuracy. Notably, while Group AbsMax improves the accuracy of models with low-rank adapters, it still underperforms compared to SLiM-Quant, which employs a single quantization parameter per tensor for greater efficiency.

A similar trend is observed for unstructured sparsity, although the performance gap between dense and sparse models is smaller across all methods. SLiM achieves a significant improvement in average accuracy, boosting results by up to 5.4% (LLaMA-2-7B) for 2:4 sparsity compared to the state-of-the-art SparseGPT and Group OPTQ. This gap further widens to 5.8% (LLaMA-2-13B) when incorporating an additional parameter-efficient fine-tuning step.

Sparse Only. To isolate the effects of sparsity on model accuracy, we conduct a series of experiments with quantization disabled. Our sparsity benchmarks include Magnitude Pruning, SparseGPT, and Wanda, along with low-rank approximations using Wanda-SVD and SLiM. We evaluate both 50% unstructured sparsity and 2:4 structured sparsity patterns in our experiments.

Table 2 presents the accuracy results for the sparse models. As anticipated, Magnitude Pruning yields the lowest accuracy. Wanda and SparseGPT achieve comparable results, though in the case of semi-structured sparsity, their performance gap with the dense model is more pronounced. Introducing low-rank adapters improves model accuracy, with SLiM being particularly effective due to its saliency-based approximation. Finally, a brief fine-tuning phase further enhances the accuracy of the low-rank approximations.

Table 1: Average zero-shot accuracy of LLaMA-2 and OPT models with pruning, 4-bit symmetric weight quantization, and 8-bit symmetric input group quantization. Wanda-SVD uses SVD directly on the compression error matrix, and Wanda-SVD + FT and SLiM + FT uses fine-tuning on low-rank adapters for 300,000 tokens. SLiM^Q quantizes the low-rank adapters after the compression (and possibly fine-tuning) process.

| Pruning Method | Weight Quantization | OPT | | | | | | | |
|------------------------|---------------------|-------------|-------------|-------------|-------------|-------------|-------------|-------------|-------------|
| | | 125M | 350M | 1.3B | 2.7B | 6.7B | 13B | 7B | 13B |
| Dense | - | 35.9 | 37.1 | 43.4 | 45.5 | 48.3 | 48.7 | 56.6 | 60.8 |
| 50% 2:4 | | | | | | | | | |
| Magnitude | AbsMax | 32.0 | 31.8 | 34.2 | 32.5 | 35.3 | 30.8 | 31.2 | 32.1 |
| SparseGPT | Group-OPTQ | 33.7 | 32.6 | 37.3 | 40.2 | 44.4 | 45.5 | 45.4 | 50.8 |
| SparseGPT | OPTQ | 31.4 | 32.9 | 31.0 | 33.9 | 39.9 | 40.0 | 31.8 | 31.6 |
| Wanda | Group AbsMax | 33.0 | 31.6 | 36.3 | 35.1 | 36.6 | 43.4 | 43.1 | 48.3 |
| Wanda | AbsMax | 31.5 | 31.3 | 31.6 | 30.7 | 30.5 | 31.2 | 32.0 | 31.3 |
| Wanda | SLiM-Quant | 31.8 | 32.1 | 34.7 | 34.3 | 38.4 | 32.8 | 30.8 | 30.7 |
| Wanda-SVD | Group AbsMax | 33.9 | 34.0 | 38.9 | 39.9 | 44.2 | 45.5 | 50.5 | 54.5 |
| Wanda-SVD | SLiM-Quant | 34.2 | 33.3 | 38.7 | 41.2 | 44.3 | 45.2 | 48.3 | 51.4 |
| Wanda-SVD + FT | SLiM-Quant | 34.0 | 34.3 | 39.6 | 42.6 | 46.1 | 47.2 | 50.8 | 55.4 |
| SLiM | Group AbsMax | 33.9 | 33.7 | 39.9 | 42.8 | 45.8 | 46.0 | 50.2 | 54.3 |
| SLiM | SLiM-Quant | 34.3 | 33.5 | 40.0 | 42.8 | 46.1 | 46.1 | 50.8 | 54.8 |
| SLiM ^Q | SLiM-Quant | 34.2 | 33.8 | 39.8 | 41.8 | 46.0 | 45.9 | 50.6 | 53.0 |
| SLiM + FT | SLiM-Quant | 34.9 | 34.5 | 41.3 | 43.5 | 46.1 | 47.3 | 50.5 | 56.6 |
| SLiM ^Q + FT | SLiM-Quant | 34.9 | 34.3 | 40.0 | 42.3 | 46.0 | 46.5 | 50.6 | 54.1 |
| 50% | | | | | | | | | |
| Unstructured | | | | | | | | | |
| Magnitude | AbsMax | 31.1 | 32.9 | 33.1 | 36.2 | 36.3 | 31.2 | 32.6 | 31.5 |
| SparseGPT | Group-OPTQ | 35.1 | 35.1 | 38.9 | 43.2 | 47.1 | 47.3 | 50.1 | 55.4 |
| SparseGPT | OPTQ | 31.4 | 34.5 | 31.2 | 37.1 | 43.2 | 44.1 | 31.7 | 32.0 |
| Wanda | Group AbsMax | 34.2 | 33.3 | 39.1 | 40.7 | 44.9 | 46.2 | 51.7 | 55.8 |
| Wanda | AbsMax | 31.5 | 32.9 | 31.0 | 32.9 | 30.5 | 31.1 | 32.7 | 31.1 |
| Wanda | SLiM-Quant | 32.8 | 33.9 | 36.0 | 36.2 | 42.7 | 32.8 | 30.4 | 30.5 |
| Wanda-SVD | Group AbsMax | 34.6 | 34.4 | 40.5 | 42.9 | 46.3 | 47.2 | 53.9 | 55.4 |
| Wanda-SVD | SLiM-Quant | 34.6 | 34.4 | 40.3 | 43.3 | 46.7 | 45.2 | 51.2 | 55.4 |
| Wanda-SVD + FT | SLiM-Quant | 35.3 | 34.8 | 41.8 | 43.8 | 47.0 | 47.9 | 53.0 | 57.3 |
| SLiM | Group AbsMax | 35.0 | 35.0 | 41.5 | 43.6 | 47.2 | 47.9 | 54.0 | 57.6 |
| SLiM | SLiM-Quant | 35.7 | 35.4 | 42.0 | 43.4 | 47.5 | 48.0 | 54.0 | 57.6 |
| SLiM ^Q | SLiM-Quant | 34.8 | 35.0 | 41.4 | 34.3 | 47.1 | 47.4 | 53.8 | 57.1 |
| SLiM + FT | SLiM-Quant | 35.7 | 35.8 | 42.3 | 44.3 | 47.3 | 48.4 | 53.2 | 57.0 |
| SLiM ^Q + FT | SLiM-Quant | 35.3 | 35.6 | 41.9 | 43.8 | 47.6 | 48.1 | 53.7 | 57.6 |

Quantized Only. To assess the effects of SLiM-Quant and the low-rank compensation in SLiM , we disable sparsity in our experiments and evaluate various quantization schemes. Specifically, we test AbsMax, OPTQ, and SLiM-Quant as the quantization methods. To improve model accuracy, we add low-rank adapters to SLiM-Quant , minimizing either the error saliency (SLiM) or the reconstruction error norm (SVD). Low-rank adapters cannot be applied to OPTQ due to its weight update rules, which conflict with minimizing the weight reconstruction error.

Table 3 summarizes the results of our quantization experiments. As expected, AbsMax produces the highest error among the quantization methods. While SLiM-Quant addresses some of the limitations of AbsMax, it still struggles to fully recover from accuracy loss. OPTQ achieves higher

Table 2: Average zero-shot accuracy of LLaMA-2 and OPT models with pruning. The quantization is disabled in this experiment.

| Pruning Method | | | OPT | | | | LLaMA-2 | | |
|-------------------------|-------------|-------------|-------------|-------------|-------------|-------------|-------------|-------------|--|
| | 125M | 350M | 1.3B | 2.7B | 6.7B | 13B | 7B | 13B | |
| Dense | 35.9 | 37.1 | 43.4 | 45.5 | 48.3 | 48.7 | 56.6 | 60.8 | |
| 50% 2:4 | | | | | | | | | |
| Magnitude | 32.6 | 31.8 | 35.4 | 33.9 | 36.4 | 30.7 | 31.2 | 32.0 | |
| SparseGPT | 33.8 | 33.2 | 37.7 | 41.3 | 45.2 | 45.6 | 47.3 | 52.3 | |
| Wanda | 34.0 | 32.5 | 38.3 | 40.5 | 43.2 | 44.1 | 46.1 | 49.7 | |
| Wanda-SVD | 34.1 | 34.1 | 40.4 | 42.8 | 46.0 | 45.9 | 51.6 | 55.8 | |
| Wanda-SVD + FT | 34.8 | 34.5 | 41.3 | 43.4 | 46.5 | 47.2 | 52.4 | 56.9 | |
| SLiM | 34.5 | 32.9 | 40.7 | 43.1 | 46.4 | 46.3 | 51.4 | 56.1 | |
| SLiM + FT | 35.1 | 34.9 | 41.5 | 43.8 | 46.5 | 47.3 | 51.6 | 56.4 | |
| 50% Unstructured | | | | | | | | | |
| Magnitude | 33.3 | 33.7 | 34.0 | 40.6 | 35.8 | 30.9 | 32.6 | 31.9 | |
| SparseGPT | 35.5 | 35.1 | 39.6 | 43.5 | 47.4 | 47.8 | 53.3 | 57.3 | |
| Wanda | 35.0 | 34.5 | 41.1 | 42.9 | 46.5 | 46.8 | 52.7 | 57.2 | |
| Wanda-SVD | 35.3 | 35.2 | 41.9 | 44.1 | 47.5 | 47.8 | 54.9 | 58.5 | |
| Wanda-SVD + FT | 35.74 | 35.7 | 42.7 | 44.6 | 47.8 | 48.4 | 54.9 | 58.7 | |
| SLiM | 35.2 | 35.1 | 42.0 | 44.1 | 47.7 | 48.2 | 55.0 | 58.8 | |
| SLiM + FT | 35.9 | 35.7 | 42.5 | 44.7 | 47.7 | 48.4 | 55.0 | 58.8 | |

accuracy than both AbsMax and SLiM-Quant , but its inability to incorporate low-rank adapters limits its effectiveness at lower bitwidths. Both the SVD and SLiM low-rank adapters enhance the accuracy of SLiM-Quant , with SLiM outperforming SVD in most cases due to its saliency-based approximation. It is noteworthy that in some rare cases, Group-AbsMax with low-rank adapters outperforms SLiM-Quant with low-rank adapters because it uses significantly more quantization parameters.

Table 3: Average zero-shot accuracy of LLaMA-2 and OPT models with quantization. The sparsity is disabled in this experiment.

| Quantization Method | Low-rank Adapter | | | OPT | | | | LLaMA-2 | | |
|---------------------|------------------|-------------|-------------|-------------|-------------|-------------|-------------|-------------|-------------|--|
| | | 125M | 350M | 1.3B | 2.7B | 6.7B | 13B | 7B | 13B | |
| Dense | - | 35.9 | 37.1 | 43.4 | 45.5 | 48.3 | 48.7 | 56.6 | 60.8 | |
| AbsMax | - | 30.7 | 34.0 | 31.2 | 31.6 | 30.3 | 31.4 | 32.4 | 31.9 | |
| Group-OPTQ | - | 35.5 | 36.2 | 42.5 | 44.5 | 47.7 | 48.2 | 53.3 | 59.6 | |
| OPTQ | - | 31.4 | 36.0 | 31.5 | 37.3 | 43.3 | 45.1 | 31.2 | 31.5 | |
| Group-AbsMax | - | 35.1 | 36.0 | 41.8 | 44.3 | 46.9 | 48.5 | 56.0 | 59.9 | |
| Group-AbsMax | SVD | 35.1 | 36.6 | 42.4 | 44.8 | 47.7 | 48.5 | 56.4 | 60.2 | |
| Group-AbsMax | SLiM | 35.6 | 36.8 | 42.6 | 44.8 | 47.9 | 48.8 | 56.2 | 60.2 | |
| SLiM-Quant | - | 32.0 | 36.5 | 36.2 | 40.0 | 30.3 | 37.8 | 31.0 | 30.5 | |
| SLiM-Quant | SVD | 35.5 | 35.9 | 42.4 | 44.9 | 47.8 | 48.2 | 55.8 | 60.5 | |
| SLiM-Quant | SVD + FT | 35.9 | 36.4 | 43.2 | 45.5 | 48.2 | 48.7 | 56.0 | 60.4 | |
| SLiM-Quant | SLiM | 35.6 | 36.5 | 42.7 | 45.4 | 48.3 | 48.4 | 56.0 | 60.2 | |
| SLiM-Quant | SLiM + FT | 35.7 | 36.5 | 43.2 | 45.6 | 48.3 | 48.9 | 55.8 | 60.4 | |

Fine-tuning Costs. Fine-tuning compressed models can help recover lost accuracy. However, fine-tuning quantized weights presents challenges due to the discrete nature of the weights. The most commonly used approach for addressing these challenges, and one that has shown promising results, is the straight-through estimator (STE) (Bengio et al., 2013). In this method, during the backward pass and optimization step, the weights are treated as continuous, allowing for effective fine-tuning despite the quantization.

In addition to the challenges posed by discrete values during fine-tuning, the high parameter count of the models leads to time-consuming computations and substantial memory costs. In our experiments, we measured the time required to fine-tune the models under various conditions. For models with low-rank adapters, the quantized weights are frozen, allowing only the low-rank adapters to be fine-tuned. This approach results in a more parameter-efficient fine-tuning strategy, reducing both memory and computational costs. When no low-rank adapter is employed, the straight-through estimator (STE) is used for fine-tuning the quantized weights. Table 4 summarizes the fine-tuning results for 300,000 tokens from the C4 dataset, with a batch size of 64 and a sequence length of 1024 on a single H100 GPU. The fine-tuning costs for models without low-rank adapters range from 12 hours for 125M parameter models to over 36 days for 13B parameter models. Due to these high costs, we faced challenges completing the fine-tuning with our limited resources. In contrast, utilizing low-rank adapters and freezing the sparse quantized weights enables a much more parameter-efficient fine-tuning method, making it feasible for us to report the accuracy results for these cases in Table 1.

Table 4: The required time for fine-tuning the models with a single H100 GPU on 300,000 tokens from the C4 dataset with a batch size of 64 and a sequence length of 1024.

| Pruning Method | Weight Quantization | OPT | | | | | | LLaMA-2 | |
|----------------|---------------------|------|------|------|------|------|------|---------|------|
| | | 125M | 350M | 1.3B | 2.7B | 6.7B | 13B | 7B | 13B |
| Magnitude | AbsMax | | | | | | | | |
| SparseGPT | OPTQ | 12h | 43h | 164h | 361h | 866h | 867h | 842h | 844h |
| Wanda | AbsMax | | | | | | | | |
| Wanda-SVD | SLiM-Quant | 1.5h | 3h | 6h | 8h | 16h | 18h | 14h | 14h |
| SLiM + FT | SLiM-Quant | | | | | | | | |

Additional Experiments. In the appendix, we provide additional experiments for a comprehensive evaluation. **Compression Costs** (Appendix C) examines the time required to compress models of varying sizes using different methods. **Inference Speedup** (Appendix D) evaluates the performance gains during inference, highlighting the efficiency improvements achieved by our approach. **Rank Analysis** (Appendix E) investigates the computational and memory costs of different ranks in low-rank adapter methods, along with their impact on model accuracy. Finally, **Effects of Calibration Sample Count** (Appendix F) analyzes how varying the number of calibration samples affects accuracy in methods that require calibration.

5 CONCLUSION, LIMITATIONS, AND FUTURE WORK

In this paper, we introduced SLiM, a one-shot quantized sparse plus low-rank approximation method for large language models, designed to balance memory efficiency and accuracy. By leveraging symmetric quantization, sparsity, and saliency-based low-rank adapters, SLiM achieves significant reductions in both memory and computational costs while maintaining competitive performance. Our method demonstrates improved accuracy, particularly for models with structured sparsity patterns like 2:4 sparsity, compared to state-of-the-art approaches.

SLiM relies on current available libraries all of which lack support for advanced quantization schemes like 2:4 mixed 8-bit and 4-bit group quantization. Additionally, low-rank adapters, while effective, introduce overheads. Future work will focus on developing efficient kernels for 2:4 group quantization and compressing low-rank adapters to further optimize memory and speed.

REFERENCES

- Dan Alistarh, Demjan Grubic, Jerry Li, Ryota Tomioka, and Milan Vojnovic. Qsgd: Randomized quantization for communication-efficient stochastic gradient descent. In *Proceedings of NIPS*, volume 2017, 2017.
- Yoshua Bengio, Nicholas Léonard, and Aaron Courville. Estimating or propagating gradients through stochastic neurons for conditional computation. *arXiv preprint arXiv:1308.3432*, 2013.
- Yonatan Bisk, Rowan Zellers, Jianfeng Gao, Yejin Choi, et al. Piqa: Reasoning about physical commonsense in natural language. In *Proceedings of the AAAI conference on artificial intelligence*, volume 34, pp. 7432–7439, 2020.
- Tom Brown, Benjamin Mann, Nick Ryder, Melanie Subbiah, Jared D Kaplan, Prafulla Dhariwal, Arvind Neelakantan, Pranav Shyam, Girish Sastry, Amanda Askell, et al. Language models are few-shot learners. *Advances in neural information processing systems*, 33:1877–1901, 2020.
- Peter Clark, Isaac Cowhey, Oren Etzioni, Tushar Khot, Ashish Sabharwal, Carissa Schoenick, and Oyvind Tafjord. Think you have solved question answering? try arc, the ai2 reasoning challenge. *arXiv preprint arXiv:1803.05457*, 2018.
- Tim Dettmers, Artidoro Pagnoni, Ari Holtzman, and Luke Zettlemoyer. QLoRA: Efficient Finetuning of Quantized LLMs. *arXiv preprint arXiv:2305.14314*, 2023.
- Elias Frantar and Dan Alistarh. Sparsegpt: Massive language models can be accurately pruned in one-shot. In *International Conference on Machine Learning*, pp. 10323–10337. PMLR, 2023.
- Elias Frantar, Saleh Ashkboos, Torsten Hoefler, and Dan Alistarh. Optq: Accurate quantization for generative pre-trained transformers. In *The Eleventh International Conference on Learning Representations*, 2022.
- Leo Gao, Jonathan Tow, Baber Abbasi, Stella Biderman, Sid Black, Anthony DiPofi, Charles Foster, Laurence Golding, Jeffrey Hsu, Alain Le Noac’h, Haonan Li, Kyle McDonell, Niklas Muenighoff, Chris Ociepa, Jason Phang, Laria Reynolds, Hailey Schoelkopf, Aviya Skowron, Lintang Sutawika, Eric Tang, Anish Thite, Ben Wang, Kevin Wang, and Andy Zou. A framework for few-shot language model evaluation, 07 2024. URL <https://zenodo.org/records/12608602>.
- Amir Gholami, Sehoon Kim, Zhen Dong, Zhewei Yao, Michael W Mahoney, and Kurt Keutzer. A survey of quantization methods for efficient neural network inference. In *Low-Power Computer Vision*, pp. 291–326. Chapman and Hall/CRC, 2022.
- Park Gunho, Park Baeseong, Kwon Se Jung, Kim Byeongwook, Lee Youngjoo, and Lee Dongsoo. nuqmm: Quantized matmul for efficient inference of large-scale generative language models. *arXiv preprint arXiv:2206.09557*, 2022.
- Han Guo, Philip Greengard, Eric P Xing, and Yoon Kim. LQ-LoRA: Low-rank Plus Quantized Matrix Decomposition for Efficient Language Model Finetuning. *arXiv preprint arXiv:2311.12023*, 2023.
- Song Han, Jeff Pool, John Tran, and William Dally. Learning both weights and connections for efficient neural network. *Advances in neural information processing systems*, 28, 2015.
- Babak Hassibi, David Stork, and Gregory Wolff. Optimal brain surgeon: Extensions and performance comparisons. *Advances in neural information processing systems*, 6, 1993.
- Dan Hendrycks, Collin Burns, Steven Basart, Andy Zou, Mantas Mazeika, Dawn Song, and Jacob Steinhardt. Measuring massive multitask language understanding. *arXiv preprint arXiv:2009.03300*, 2020.
- Benoit Jacob, Skirmantas Kligys, Bo Chen, Menglong Zhu, Matthew Tang, Andrew Howard, Hartwig Adam, and Dmitry Kalenichenko. Quantization and training of neural networks for efficient integer-arithmetic-only inference. In *Proceedings of the IEEE conference on computer vision and pattern recognition*, pp. 2704–2713, 2018.

- Yann LeCun, John Denker, and Sara Solla. Optimal brain damage. *Advances in neural information processing systems*, 2, 1989.
- Yixiao Li, Yifan Yu, Qingru Zhang, Chen Liang, Pengcheng He, Weizhu Chen, and Tuo Zhao. Lospase: Structured compression of large language models based on low-rank and sparse approximation. In *International Conference on Machine Learning*, pp. 20336–20350. PMLR, 2023.
- Ji Lin, Jiaming Tang, Haotian Tang, Shang Yang, Wei-Ming Chen, Wei-Chen Wang, Guangxuan Xiao, Xingyu Dang, Chuang Gan, and Song Han. Awq: Activation-aware weight quantization for on-device llm compression and acceleration. *Proceedings of Machine Learning and Systems*, 6: 87–100, 2024.
- I Loshchilov. Decoupled weight decay regularization. *arXiv preprint arXiv:1711.05101*, 2017.
- Stephen Merity, Caiming Xiong, James Bradbury, and Richard Socher. Pointer sentinel mixture models, 2016.
- Todor Mihaylov, Peter Clark, Tushar Khot, and Ashish Sabharwal. Can a suit of armor conduct electricity? a new dataset for open book question answering. *arXiv preprint arXiv:1809.02789*, 2018.
- Asit Mishra, Jorge Albericio Latorre, Jeff Pool, Darko Stosic, Dusan Stosic, Ganesh Venkatesh, Chong Yu, and Paulius Micikevicius. Accelerating sparse deep neural networks. *arXiv preprint arXiv:2104.08378*, 2021.
- Mohammad Mozaffari, Sikan Li, Zhao Zhang, and Maryam Mehri Dehnavi. MKOR: Momentum-Enabled Kronecker-Factor-Based Optimizer Using Rank-1 Updates. In *NeurIPS*, 2023.
- Mahdi Nikdan, Soroush Tabesh, and Dan Alistarh. Rosa: Accurate parameter-efficient fine-tuning via robust adaptation. *arXiv preprint arXiv:2401.04679*, 2024.
- NVIDIA Corporation. NVIDIA cuSPARSELt. <https://docs.nvidia.com/cuda/cusparselt/index.html>, a.
- NVIDIA Corporation. NVIDIA CUTLASS. <https://github.com/NVIDIA/cutlass>, b.
- Eunhyeok Park, Sungjoo Yoo, and Peter Vajda. Value-aware quantization for training and inference of neural networks. In *Proceedings of the European Conference on Computer Vision (ECCV)*, pp. 580–595, 2018.
- Alec Radford, Jeffrey Wu, Rewon Child, David Luan, Dario Amodei, Ilya Sutskever, et al. Language models are unsupervised multitask learners. *OpenAI blog*, 1(8):9, 2019.
- Colin Raffel, Noam Shazeer, Adam Roberts, Katherine Lee, Sharan Narang, Michael Matena, Yanqi Zhou, Wei Li, and Peter J. Liu. Exploring the limits of transfer learning with a unified text-to-text transformer. *arXiv e-prints*, 2019.
- Babak Rokh, Ali Azarpeyvand, and Alireza Khanteymooi. A comprehensive survey on model quantization for deep neural networks in image classification. *ACM Transactions on Intelligent Systems and Technology*, 14(6):1–50, 2023.
- Keisuke Sakaguchi, Ronan Le Bras, Chandra Bhagavatula, and Yejin Choi. Winogrande: An adversarial winograd schema challenge at scale. *Communications of the ACM*, 64(9):99–106, 2021.
- Victor Sanh, Thomas Wolf, and Alexander Rush. Movement pruning: Adaptive sparsity by fine-tuning. *Advances in neural information processing systems*, 33:20378–20389, 2020.
- Sidak Pal Singh and Dan Alistarh. Woodfisher: Efficient second-order approximation for neural network compression. *Advances in Neural Information Processing Systems*, 33:18098–18109, 2020.
- Mingjie Sun, Zhuang Liu, Anna Bair, and J Zico Kolter. A simple and effective pruning approach for large language models. *arXiv preprint arXiv:2306.11695*, 2023.

- Mirac Suzgun, Nathan Scales, Nathanael Schärli, Sebastian Gehrmann, Yi Tay, Hyung Won Chung, Aakanksha Chowdhery, Quoc V Le, Ed H Chi, Denny Zhou, , and Jason Wei. Challenging big-bench tasks and whether chain-of-thought can solve them. *arXiv preprint arXiv:2210.09261*, 2022.
- Hugo Touvron, Louis Martin, Kevin Stone, Peter Albert, Amjad Almahairi, Yasmine Babaei, Nikolay Bashlykov, Soumya Batra, Prajjwal Bhargava, Shruti Bhosale, et al. Llama 2: Open foundation and fine-tuned chat models. *arXiv preprint arXiv:2307.09288*, 2023.
- Shibo Wang and Pankaj Kanwar. BFloat16: The secret to high performance on Cloud TPUs. <https://cloud.google.com/blog/products/ai-machine-learning/bfloat16-the-secret-to-high-performance-on-cloud-tpus>.
- T Wolf. Huggingface’s transformers: State-of-the-art natural language processing. *arXiv preprint arXiv:1910.03771*, 2019.
- Guangxuan Xiao, Ji Lin, Mickael Seznec, Hao Wu, Julien Demouth, and Song Han. Smoothquant: Accurate and efficient post-training quantization for large language models. In *International Conference on Machine Learning*, pp. 38087–38099. PMLR, 2023.
- Susan Zhang, Stephen Roller, Naman Goyal, Mikel Artetxe, Moya Chen, Shuohui Chen, Christopher Dewan, Mona Diab, Xian Li, Xi Victoria Lin, et al. Opt: Open pre-trained transformer language models. *arXiv preprint arXiv:2205.01068*, 2022.
- Jeffrey Zhou, Tianjian Lu, Swaroop Mishra, Siddhartha Brahma, Sujoy Basu, Yi Luan, Denny Zhou, and Le Hou. Instruction-following evaluation for large language models. *arXiv preprint arXiv:2311.07911*, 2023.

Appendix

Table of Contents

| | | |
|----------|--|-----------|
| A | Language Modeling Experiments | 14 |
| B | Fine-tuning Hyperparameters | 14 |
| C | Compression Costs | 14 |
| D | Inference Speedup | 15 |
| E | Rank Analysis | 16 |
| F | Effects of Calibration Sample Count | 17 |

A LANGUAGE MODELING EXPERIMENTS

We have tested all the benchmarks discussed in Section 4 on a language modeling task on the Wiki-Text2 (Merity et al., 2016) dataset. Table 5 summarizes the results for different pruning and quantization approaches when using 4-bit weight and 8-bit group input quantization. Similar to Section 4, SLiM outperforms all the previous methods, including SparseGPT with Group OPTQ. Using saliency based methods for low-rank adapters is also improving the perplexity of the models in comparison to Wanda-SVD. Additionally, a short fine-tuning step can improve the perplexity of the models significantly.

B FINE-TUNING HYPERPARAMETERS

For fine-tuning the models, we utilized the Hugging Face Trainer (Wolf, 2019). The ADAMW (Loshchilov, 2017) optimizer was employed during the fine-tuning process, accompanied by linear learning rate scheduling. The optimization and learning rate scheduling parameters were set to their default values in the Hugging Face Trainer. To prevent numerical overflow and divergence, we used BFloat-16 data types (Wang & Kanwar) available on NVIDIA H100 GPUs during fine-tuning. The training was conducted with a local batch size of 1 and a gradient accumulation factor of 64 to reduce memory overhead. Weight updates for the sparse and/or quantized weights, as well as the corresponding biases, were disabled. Due to our limited resources, we did not tune any of the hyperparameters aimed at improving fine-tuning speed or accuracy; tuning these parameters is planned for future work.

C COMPRESSION COSTS

An important factor in model compression is the computational cost of the chosen method. In terms of memory usage, all approaches can be adapted to store only a single layer of the model in the GPU’s global memory at a time, allowing them to be compressed on a single GPU. However, the computational costs vary depending on the complexity of the method. Techniques like Wanda, which rely solely on matrix multiplication, are significantly faster than more complex methods like SparseGPT, which computes the inverse Hessian matrix for each layer. Adding low-rank adapters in Wanda-SVD and SLiM requires performing singular value decomposition (SVD) on different matrices, resulting in a computational complexity similar to that of SparseGPT. Table 6 summarizes the time required to compress various models using the methods discussed in this paper. Generally, methods incorporating low-rank adapters (SLiM and Wanda-SVD) have higher complexity. However, SparseGPT’s compression time is comparable to methods with low-rank adapters, despite only

Table 5: Perplexity of LLaMA-2 and OPT models with pruning, 4-bit symmetric weight quantization, and 8-bit symmetric input group quantization on WikiText2 dataset language modeling task. Wanda-SVD uses SVD directly on the compression error matrix, and Wanda-SVD + FT and SLiM + FT uses fine-tuning on low-rank adapters for 300,000 tokens.

| Pruning Method | Weight Quantization | OPT | | | | | | LLaMA-2 | |
|---------------------|---------------------|-------------|-------------|-------------|-------------|-------------|-------------|------------|------------|
| | | 125M | 350M | 1.3B | 2.7B | 6.7B | 13B | 7B | 13B |
| Dense | - | 27.7 | 22.0 | 14.6 | 12.5 | 10.9 | 10.1 | 5.1 | 4.6 |
| 50% 2:4 | | | | | | | | | |
| Magnitude | AbsMax | 6.2e3 | 9.1e2 | 2.1e3 | 1.5e3 | 436.3 | 4.1e4 | 9.1e4 | 1.1e5 |
| SparseGPT | Group-OPTQ | 78.6 | 62.3 | 27.1 | 18.7 | 15.4 | 12.9 | 15.2 | 8.3 |
| SparseGPT | OPTQ | 6.7e3 | 77.2 | 762.3 | 52.1 | 21.1 | 15.36 | 7.4 | 1.2e5 |
| Wanda | AbsMax | 6.2e3 | 412.6 | 1.0e4 | 1.0e4 | 8.8e3 | 8.2e3 | 8.1e4 | 6.6e4 |
| Wanda | SLiM-Quant | 308.4 | 145.7 | 1.3e3 | 441.5 | 65.2 | 2.3e3 | 5.2e5 | 7.6e4 |
| Wanda-SVD | SLiM-Quant | 83.6 | 60.7 | 27.4 | 21.3 | 14.7 | 13.2 | 8.2 | 7.1 |
| Wanda-SVD + FT | SLiM-Quant | 54.5 | 42.1 | 21.1 | 16.3 | 13.4 | 12.6 | 7.0 | 6.0 |
| SLiM | SLiM-Quant | 58.1 | 51.7 | 20.0 | 15.8 | 12.8 | 12.1 | 7.6 | 6.6 |
| SLiM + FT | SLiM-Quant | 41.5 | 36.3 | 17.6 | 14.7 | 12.4 | 12.1 | 6.4 | 5.8 |
| 50% | | | | | | | | | |
| Unstructured | | | | | | | | | |
| Magnitude | AbsMax | 3.1e3 | 127.3 | 7.1e3 | 1.1e3 | 772.3 | 2.3e4 | 9.9e4 | 2.0e5 |
| SparseGPT | Group-OPTQ | 42.6 | 34.7 | 20.3 | 14.4 | 12.2 | 11.3 | 8.4 | 5.6 |
| SparseGPT | OPTQ | 4.8e3 | 39.4 | 463.0 | 29.7 | 15.1 | 12.7 | 1.2e4 | 8.6e4 |
| Wanda | AbsMax | 5.9e3 | 84.2 | 1.3e4 | 1.1e3 | 7.1e3 | 5.6e3 | 9.3e4 | 1.6e5 |
| Wanda | SLiM-Quant | 136.9 | 57.9 | 460.9 | 176.0 | 56.5 | 623.3 | 2.9e5 | 7.1e4 |
| Wanda-SVD | SLiM-Quant | 47.0 | 34.5 | 19.6 | 15.5 | 12.3 | 11.5 | 6.6 | 5.6 |
| Wanda-SVD + FT | SLiM-Quant | 39.2 | 29.7 | 17.8 | 14.3 | 12.3 | 11.9 | 6.1 | 5.3 |
| SLiM | SLiM-Quant | 39.7 | 32.0 | 16.7 | 13.7 | 11.5 | 10.8 | 6.2 | 5.4 |
| SLiM + FT | SLiM-Quant | 34.0 | 28.3 | 15.9 | 13.4 | 11.5 | 11.5 | 5.8 | 5.2 |

performing pruning and quantization. Notably, the saliency-based approach in SLiM does not add significant overhead compared to Wanda-SVD.

Table 6: The required compression time for different models and compression methods using a single H100 GPU.

| Pruning Method | Weight Quantization | OPT | | | | | | LLaMA-2 | |
|----------------|---------------------|------|------|------|------|------|-----|---------|-----|
| | | 125M | 350M | 1.3B | 2.7B | 6.7B | 13B | 7B | 13B |
| Magnitude | AbsMax | 1s | 1s | 1s | 1s | 2s | 4s | 2s | 4s |
| SparseGPT | OPTQ | 1m | 2m | 5m | 11m | 22m | 41m | 25m | 46m |
| Wanda | SLiM-Quant | 0.5m | 1m | 3m | 5m | 8m | 13m | 8m | 14m |
| Wanda-SVD | SLiM-Quant | 1m | 2m | 7m | 13m | 33m | 60m | 38m | 67m |
| SLiM | SLiM-Quant | 1m | 2m | 7m | 13m | 34m | 63m | 39m | 68m |

D INFERENCE SPEEDUP

Many libraries, such as CUTLASS (NVIDIA Corporation, b) and cuSPARSELt (NVIDIA Corporation, a), have implemented sparse matrix-matrix multiplication (SpMM) kernels for 2:4 sparsity.

However, to the best of our knowledge, there is no open-source code base that supports group quantization for 2:4 SpMM. Implementing such a kernel is beyond the scope of this paper, and we propose its development as part of future work. Similar to Wanda (Sun et al., 2023) and SparseGPT (Frantar & Alistarh, 2023), we focus our results on layer-wise speedups achieved using the existing code bases. Table 7 summarizes the time taken for dense, sparse, and low-rank multiplication in a linear layer, and reports the speedup achieved by SLiM across different layers in the LLaMA-2-13B model.

Table 7: The inference time of feed forward layers in LLaMA-2-13B for different weight sizes. The speedup is computed as $\frac{\text{Dense Time}}{\text{Sparse Time} + \text{Low-rank Time}}$.

| Matrix | Dense Time | Sparse Time | Low-rank Time | Speedup |
|---------------------|------------|-------------|---------------|---------|
| Q, K, V, O_{proj} | 0.96ms | 0.44ms | 0.22ms | 1.46× |
| Upsample | 2.33ms | 1.45ms | 0.39ms | 1.27× |
| Downsample | 2.19ms | 1.22ms | 0.37ms | 1.37× |

E RANK ANALYSIS

The key hyperparameter in low-rank approximation is the rank of the adapters. While increasing the rank reduces approximation error, it also leads to higher computational and memory overhead. Therefore, it is crucial to analyze the trade-off between the accuracy improvements and the overhead introduced by the chosen approximation rank.

Assuming the rank of the low-rank adapter is rd , where $r < 1$ is a fixed factor and d is the dimension of the weights in a square feed-forward layer, the low-rank adapters are represented as $\mathcal{L}, \mathcal{R}^T \in \mathbb{R}^{d \times rd}$, resulting in a memory overhead of $\mathcal{O}(2rd^2)$ for storing them. To compute $\mathcal{X}\mathcal{L}\mathcal{R}$, where $\mathcal{X} \in \mathbb{R}^{b \times d}$ is the input with a batch size of b , the computational complexity is $\mathcal{O}(2brd^2)$. Given that the original memory and computational complexity of the layer are $\mathcal{O}(d^2)$ and $\mathcal{O}(bd^2)$, respectively, the overhead introduced by the low-rank adapters becomes negligible when $r \ll 1$.

Figure E-a shows the average zero-shot accuracy of the OPT-6.7B and LLaMA-2-7B models for various ranks. As expected, increasing the rank leads to improved model accuracy. Based on these results, a rank of $r = 0.1$ provides a substantial boost in accuracy without introducing significant overhead to inference.

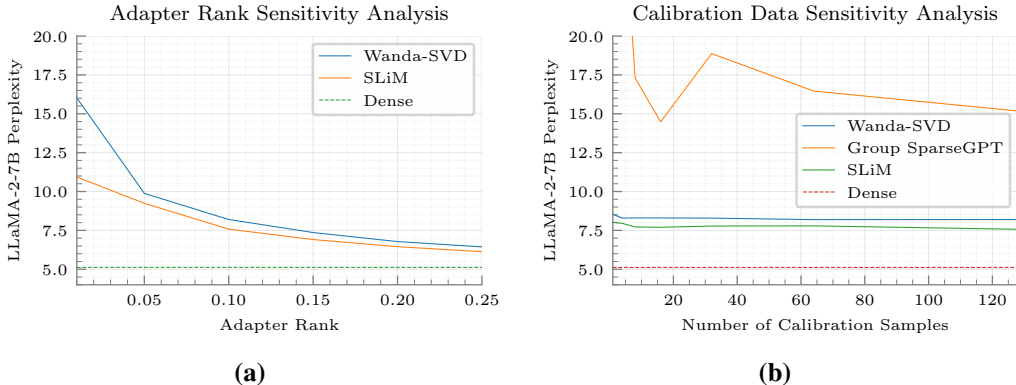


Figure 2: Sensitivity analysis for the rank of the adapter (a) and the number of calibration samples (b) for different one-shot compression methods. For Wanda-SVD and SLiM, we have used the SLiM-Quant quantization method, and for the SparseGPT, we have used the Group quantization version of OPTQ. The non-group version of OPTQ and Wanda without low-rank adapters lead to divergence, and hence are not included in this figure.

F EFFECTS OF CALIBRATION SAMPLE COUNT

Similar to SparseGPT and Wanda, SLIM leverages a set of calibration data from the C4 dataset to assess weight saliency for pruning and low-rank approximations. Figure E-b illustrates the perplexity of LLaMA-2-7B using varying numbers of calibration samples. As shown, SLIM demonstrates low sensitivity to the number of calibration samples, making it effective even in scenarios with limited data.